

## Preparation of a pristine TiO<sub>2</sub> anatase (101) surface by cleaving

This article has been downloaded from IOPscience. Please scroll down to see the full text article.

2010 J. Phys.: Condens. Matter 22 084014

(<http://iopscience.iop.org/0953-8984/22/8/084014>)

View [the table of contents for this issue](#), or go to the [journal homepage](#) for more

Download details:

IP Address: 129.252.86.83

The article was downloaded on 30/05/2010 at 07:14

Please note that [terms and conditions apply](#).

# Preparation of a pristine TiO<sub>2</sub> anatase (101) surface by cleaving

Olga Dulub and Ulrike Diebold<sup>1</sup>

Department of Physics, Tulane University, New Orleans, LA 70118, USA

E-mail: [diebold@tulane.edu](mailto:diebold@tulane.edu)

Received 9 October 2009

Published 4 February 2010

Online at [stacks.iop.org/JPhysCM/22/084014](http://stacks.iop.org/JPhysCM/22/084014)

## Abstract

A natural TiO<sub>2</sub> anatase crystal, cut to exhibit its (010) surface, was cleaved by breaking off one of its corners. The resulting sample exhibited a small, flat area ca. 2 mm<sup>2</sup> in size with a (101) orientation as confirmed by LEED. The evolution of the surface morphology was monitored with UHV-STM. After one sputtering/annealing cycle the surface is characterized by periodic ridges that run parallel to the [010] direction. The ridges are ~3 nm high and 10–15 nm wide and have a spacing of 30 nm. Interestingly, [1 $\bar{1}\bar{1}$ ]/[111]-oriented step edges are not observed, despite them having the lowest formation energy. The ridges flatten with repeated sputter/annealing cycles. After a total of three cycles a flat surface is achieved, which exhibits trapezoidal terraces that are typical for anatase (101). The importance of preparing such a pristine surface for understanding the surface structure and chemistry of TiO<sub>2</sub> anatase is discussed.

## 1. Introduction

In recent years, titanium dioxide (TiO<sub>2</sub>) has become one of the most-commonly used systems in surface science [1, 2]. This high interest is motivated by the technological importance of this versatile material. TiO<sub>2</sub> crystallizes in three main structures: rutile, anatase, and brookite. Very often technical TiO<sub>2</sub> is of anatase form. For example, the benchmark photocatalyst Degussa P-25 consists of a mixture of rutile and anatase, the TiO<sub>2</sub>-based electrode in dye-sensitized ‘Grätzel’ cells [3] is composed of anatase, and almost all TiO<sub>2</sub>-based nanomaterials have the anatase structure. Despite the high technical importance of anatase, most experimental surface studies of TiO<sub>2</sub> so far have focused on TiO<sub>2</sub> rutile. One reason for this imbalance is the difficulty in obtaining appropriate specimens. While rutile samples are readily available, the anatase crystal structure is metastable and transforms into the lowest-energy rutile phase upon high-temperature treatment. This complicates the growth of crystals large enough for a convenient sample handling.

First-principles DFT calculations have shown that the lowest-energy face of anatase is the (101) surface [4], and a Wulff construction of the equilibrium crystal shape (figure 1(a)) shows that most of the anatase surface is terminated with this surface orientation [4, 5]. Anatase may be

stabilized as a thin film; (001)-oriented films have been grown successfully on SrTiO<sub>3</sub>(001) and LaAlO<sub>3</sub>(001) [6–8], and it is possible to grow anatase (101)-oriented films on vicinal LaAlO<sub>3</sub>(110) [9, 10]. However, these growth techniques have not been widely adopted and the careful atomically-resolved STM studies so successful on rutile (110) [11–15] have not been repeated on anatase surfaces. In order to circumvent these difficulties, investigating anatase mineral samples is a viable strategy [5, 16–22]. These crystals are readily available from mineral stores, but they often contain impurities, in particular alkali and alkaline earth elements, which segregate to the surface upon the sputter/annealing cycles that are typically used to prepare flat and clean surfaces. In addition, cutting/orienting and polishing of these mineral samples is not trivial, and can result in a vicinal surface, which, for the case of anatase (101), was shown to reconstruct and facet [18].

Here we report preparation of a high-quality anatase (101) surface by *ex situ* cleaving and by minimal treatment inside our ultrahigh vacuum (UHV) chamber. The resulting surface is flat without an apparent miscut, and almost pristine.

Early work reported that TiO<sub>2</sub> ‘does not cleave but fractures’ [23], hence cleaving, which is quite successful for many other oxides, is generally not considered a viable route for producing a high-quality TiO<sub>2</sub> surface. A recent report by Bondarchuk and Lyubinetsky [24] on producing a pristine TiO<sub>2</sub>(110) surface by *in situ* cleaving has motivated us to try such a strategy for an anatase mineral sample.

<sup>1</sup> Author to whom any correspondence should be addressed.

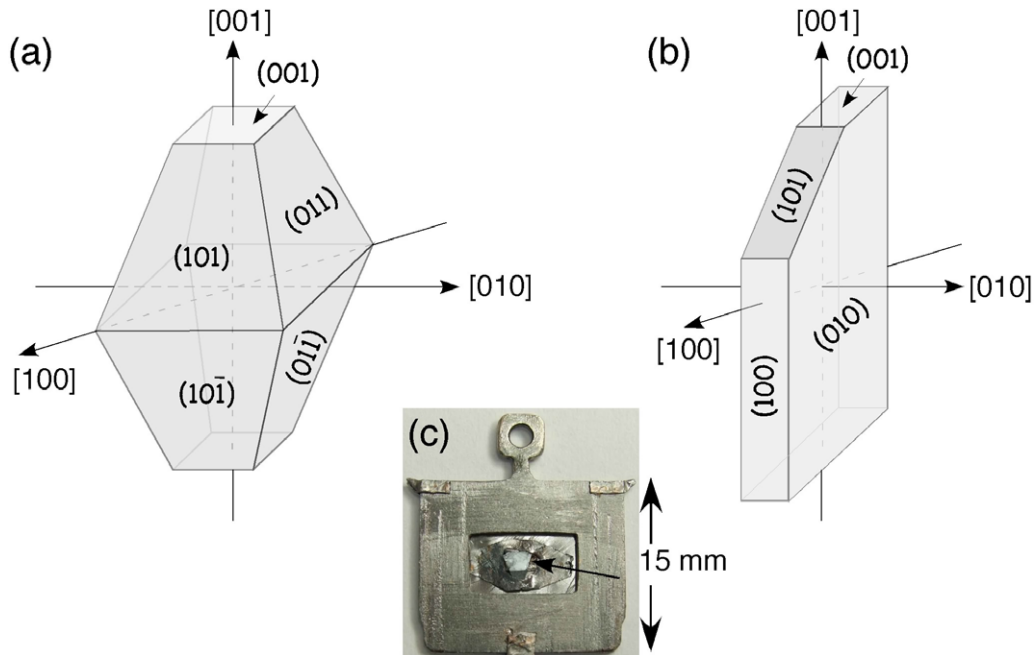


**Figure 1.** (a) Equilibrium crystal shape of anatase, adapted from [4]. (b) Schematics of the original anatase (101) sample and (c) photograph of the cleaved sample mounted on the sample holder.

## 2. Experimental details

The experiments were carried out in an ultrahigh vacuum (UHV) system with a base pressure of less than  $2 \times 10^{-10}$  mbar. The system was equipped with facilities for sample cleaning, low-energy electron diffraction (LEED), electron stimulated desorption (ESD), and STM.

The anatase (101) mineral sample was first prepared *ex situ* by cleaving. We started with a (010)-oriented crystal (figure 1(b)), and then broke off one edge by gently applying pressure with a diamond pen. The resulting sample was small in size ( $\sim 2 \text{ mm} \times 2 \text{ mm}$ ) and about half of it was visibly rough. However, an area ca.  $1 \times 2 \text{ mm}^2$  in size appeared flat and shiny. A second sample was successfully cleaved in the same manner, indicating that the cleaving procedure is reproducible. The size of the resulting samples appears mainly limited by the thickness of the original crystal (only one millimeter thick crystals were available). The first cleaved sample was mounted with Ta strips (figure 1(c)) on a sample plate (Omicron) and introduced into our UHV chamber where it was cleaned by cycles of 1 keV  $\text{Ar}^+$  ion bombardment at room temperature (1 keV Ar, 25 min, 0.5 mA) and annealing ( $640^\circ\text{C}$ , 5 min). The sample was heated radiatively, and its temperature was monitored by a thermocouple spot-welded to the sample holder.

The STM experiments were carried out using an Omicron UHV-STM-1. All STM data were collected at room temperature in constant current mode at a positive sample bias of 0.8–2.5 V and with a feedback current of 0.4–4 nA. STM tips (electrochemically etched from a 0.25 mm W wire) were cleaned by argon sputtering and by applying voltage pulses during operation.

## 3. Results and discussion

After flashing the sample once to  $500^\circ\text{C}$ , a faint LEED pattern with a high background was observed. After one cycle of sputtering and annealing the flat portion was inspected by LEED and showed a sharp  $(1 \times 1)$  pattern with split spots (inset figure 2(a-2)), while STM showed a surface with long, parallel ridges (figure 2(a-1)). These ridges run parallel to the crystallographic [010] direction and are  $\sim 3 \text{ nm}$  high, 10–15 nm wide, and are spaced roughly 30 nm apart. A small-scale image of the same sample (figure 2(a-3)) shows that it consists of narrow terraces with predominantly [010]-oriented step edges.

After another sputter/annealing cycle (figure 2(b)), the ridges widen and the surface flattens. A few of the trapezoidal islands that are typical for anatase (101) [19] appear in the medium-scale STM image (figure 2(b-2)). After one more sputter/annealing cycle the ridges have mostly disappeared (figure 2(c)). The surface now consists of flat terraces, with well-defined trapezoidal terraces on top, and a few triangular holes. The terraces are considerably larger (10–150 nm) than the terraces of the previously investigated cut-and-polished anatase samples (5–20 nm) [1]. All step edges are monoatomic (3.8 Å high).

This surface is of very high quality, and atomically-resolved images are easily obtained (figure 3). The surface shows two types of atomic-sized features that are not part of the regular, undisturbed lattice: a center black spot with two neighboring brighter spots (one is marked with a circle in figure 3) and faint, large-scale (a few nm) protrusions.

The black spots were assigned as water molecules in [16]. On  $\text{TiO}_2$  rutile (110) and (011)- $2 \times 1$  samples, an O-deficient sample results in surface point defects (oxygen vacancies) that are easily hydroxylated by exposure to water in the

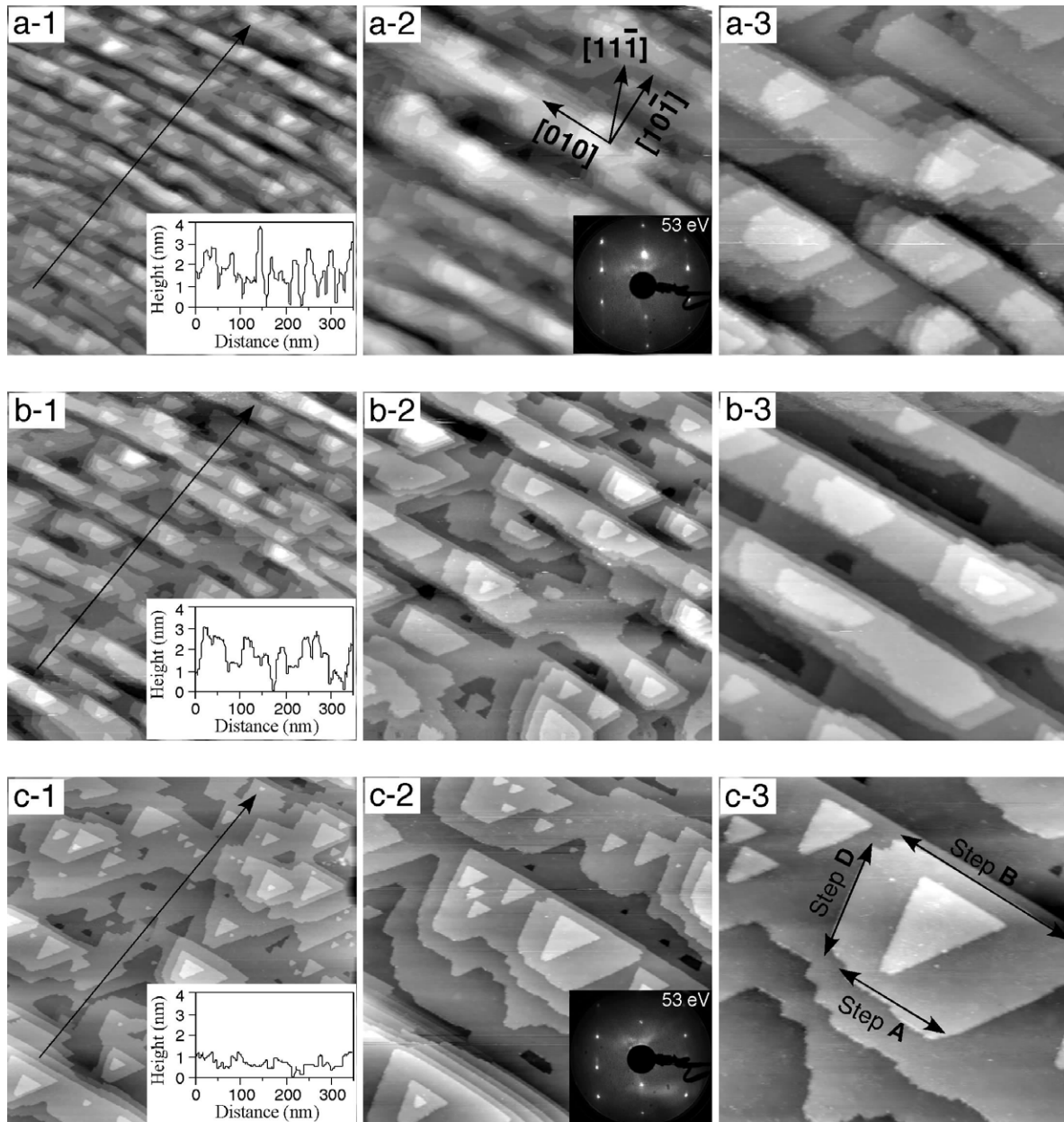


**Figure 2.** STM images of an  $\text{TiO}_2$  anatase (101) surface, cleaved *ex situ* and subjected to (a) one, (b) two, and (c) three cycles of sputtering (1 keV Ar, 25 min) and annealing (640 °C, 5 min). For each row (a)–(c), images 1, 2, and 3 cover an area of  $350 \times 350 \text{ nm}^2$ ,  $200 \times 200 \text{ nm}^2$ , and  $100 \times 100 \text{ nm}^2$ , respectively.

residual gas of UHV chambers [12, 15, 27–30]. On (perfect) anatase (101), in contrast, water adsorbs molecularly on and desorbs below room temperature [21, 26]. Another important difference to rutile is that on anatase (101) oxygen vacancies reside predominantly in subsurface sites rather than on the surface [17, 31]. Adsorbed water is stabilized by the presence of such subsurface defects [25]. Water is more strongly bound above subsurface defects on anatase (101) [25], and we take the (relatively low) number of water molecules in figure 3 as a measure of the number of subsurface defect sites that had been introduced during the previous sputter/annealing cycles. We estimated the density of these sites at  $\sim 0.005 \text{ ML}$ , where one ML is defined as the number of  $\text{Ti}_{5c}-\text{O}_{2c}$  sites on a perfect (101) surface.

The second feature, the large-scale ‘bumps’ in figure 3, change their contrast with tunneling parameters, indicating that they are due to charged, subsurface species [32]. Extensive x-ray photoemission spectroscopy (XPS) scans did not reveal any contaminants, and the Ti 2p core levels indicates stoichiometric  $\text{TiO}_2$  [17]. The number of the bumps did not increase with sputtering/annealing cycles, hence it is likely that they are due to impurities in the mineral sample with a concentration of less than  $\sim 0.05 \text{ at.}\%$ .

Previous STM and DFT investigations on anatase (101) have analyzed the formation energy of step edges on anatase (101) [19]. This surface does not have mirror symmetry along the [010] direction (the direction of the rows). This results in two different [010]-oriented step edges that have

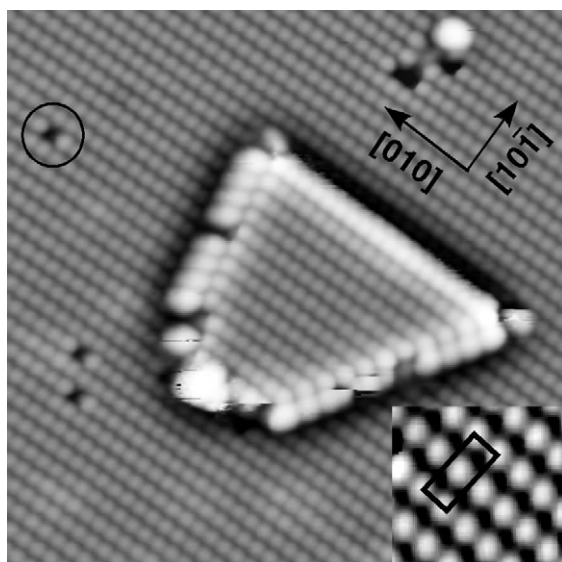


**Figure 3.** Atomically-resolved STM image ( $150 \text{ \AA} \times 150 \text{ \AA}$ ) of an anatase (101) surface, prepared as in figure 2(c). An adsorbed water molecule is circled and the centered unit cell is outlined in the inset.

slightly different formation energy. It was argued in [19] that the step edge formation energy scales with the surface energy of the associated step edge facet. Steps with the lowest formation energy ( $0.04 \text{ eV \AA}^{-1}$ ) are oriented parallel to  $[1\bar{1}\bar{1}]/[11\bar{1}]$  and have (101)-oriented step facets. These were termed ‘step-D’ in [19] and form the sides of the trapezoidal islands in figure 2(c). The [010]-oriented step-B (top side of the islands) has a step formation energy of  $0.10 \text{ eV \AA}^{-1}$ , a little higher than that of step-A ( $0.13 \text{ eV}$ ) at the opposite side (a Wulff construction based on DFT-derived step edge energies predicted a triangular shape [19], as is observed for the monoatomic holes in figure 2(c). It was argued that the formation energy of corners might change the energetics of the systems in such a way that trapezoids become the favored shape for terraces). It is interesting to note that cleaving the anatase surface does not readily result in the formation of step edges with the lowest energy. The ridges in figure 2(a) are terminated by steps-B on one side and steps-A at the other side. Only with repeated heating do the terraces assume a shape that is consistent with the energetics of the system. Apparently the fracturing process, rather than the energetics of step edge formation, is responsible for the morphology of a cleaved anatase (101) surface.

#### 4. Summary

In summary, we have shown how an anatase (101) surface can be prepared by breaking off an edge from an (010)-oriented  $\text{TiO}_2$  anatase sample. Cleaving results in a surface with a morphology that is far from its lowest-energy configuration. After a minimal further treatment (a total of three sputtering/annealing cycles), an almost pristine anatase (101) surface is obtained. The resulting surface is non-vicinal, and while the usable area is small, this method is well-suited for producing a sample that is amenable to high-quality STM measurements.

#### Acknowledgments

This work was supported by the NSF (CHE-0715576) and DoE-BES (DE-FG02-05ER15702).

#### References

- [1] Diebold U 2003 *Surf. Sci. Rep.* **48** 53–229
- [2] Pang C, Lindsay R and Thornton G 2008 *Chem. Soc. Rev.* **37** 2328–53
- [3] Grätzel M 2001 *Nature* **414** 338
- [4] Lazzeri M, Vittadini A and Selloni A 2001 *Phys. Rev. B* **63** 155409
- [5] Diebold U, Ruzycki N, Herman G S and Selloni A 2003 *Catal. Today* **85** 93–100
- [6] Liang Y, Gan S, Chambers S A and Altman E I 2001 *Phys. Rev. B* **63** 235402
- [7] Chambers S A 2000 *Surf. Sci. Rep.* **39** 105
- [8] Tanner R E, Sasahara A, Liang Y, Altman E I and Onishi H 2002 *J. Phys. Chem. B* **106** 8211–22
- [9] Gao W and Altman E I 2006 *Surf. Sci.* **600** 2572–80
- [10] Gao W, Klie R and Altman E I 2005 *Thin Solid Films* **485** 115–25
- [11] Teobaldi G, Hofer W, Bikondoa O, Pang C, Cabailh G and Thornton G 2007 *Chem. Phys. Lett.* **437** 73–8
- [12] Bikondoa O, Pang C, Ithnin R, Muryn C, Onishi H and Thornton G 2006 *Nat. Mater.* **5** 189–92
- [13] Zhang Z, Bondarchuk O, Kay B, White J M and Dohnalek Z 2006 *J. Phys. Chem. B* **110** 21840–5
- [14] Wendt S, Matthiesen J, Schaub R, Vestergaard E, Lægsgaard E, Besenbacher F and Hammer B 2006 *Phys. Rev. Lett.* **96** 066107
- [15] Dulub O, Batzill M, Solovev S, Loginova E, Alchagirov A, Madey T and Diebold U 2007 *Science* **317** 1052–6
- [16] He Y, Tilocca A, Dulub O, Selloni A and Diebold U 2009 *Nat. Mater.* **8** 585–9
- [17] He Y, Dulub O, Cheng H, Selloni A and Diebold U 2009 *Phys. Rev. Lett.* **102** 106105
- [18] Li S, Dulub O and Diebold U 2008 *J. Phys. Chem. C* **112** 16166–70
- [19] Gong X, Selloni A, Batzill M and Diebold U 2006 *Nat. Mater.* **5** 665–70
- [20] Ruzycki N, Herman G S, Boatner L A and Diebold U 2003 *Surf. Sci.* **529** L239–44
- [21] Herman G S, Dohnalek Z, Ruzycki N and Diebold U 2003 *J. Phys. Chem. B* **107** 2788–95
- [22] Gong X Q, Selloni A, Dulub O, Jacobson P and Diebold U 2008 *J. Am. Chem. Soc.* **130** 370–81
- [23] Henrich V E and Cox P A 1994 *The Surface Science of Metal Oxides* (Cambridge: Cambridge University Press)
- [24] Bondarchuk O and Lyubinetsky I 2007 *Rev. Sci. Instrum.* **78** 113907
- [25] Aschauer U, He Y B, Cheng H, Li S C, Selloni A and Diebold U 2009 at press
- [26] Tilocca A and Selloni A 2004 Vertical and lateral order in adsorbed water layers on anatase  $\text{TiO}_2(101)$  *Langmuir* **20** 8379–84
- [27] Henderson M A 1996 *Surf. Sci.* **355** 151–66
- [28] Brinkley D, Dietrich M, Engel T, Farrall P, Gantner G, Schafer A and Szuchmacher A 1998 *Surf. Sci.* **395** 292–306
- [29] Wendt S, Schaub R, Matthiesen J, Vestergaard E, Wahlström E, Rasmussen M, Thostrup P, Molina L, Lægsgaard E and Stensgaard I 2005 *Surf. Sci.* **598** 226–45
- [30] Dulub O, Valentin C, Selloni A and Diebold U 2006 *Surf. Sci.* **600** 4407–17
- [31] Cheng H and Selloni A 2009 *Phys. Rev. B* **79** 092101
- [32] Ebert P 1999 *Surf. Sci. Rep.* **33** 121–303